Integrative Biology

Accepted Manuscript

ROYAL SOCIETY OF CHEMISTRY

www.rsc.org/ibiology

Effect of adhesion and chemokine presentation on T-lymphocyte haptokinesis

George A. Dominguez[1] and Daniel A. Hammer[1,2,*]

[1.]Department of Bioengineering, University of Pennsylvania, 210 S. 33rd St, Philadelphia, PA 19104
[2.]Department of Chemical and Biomolecular Engineering, University of Pennsylvania, 220 S. 33rd St, Philadelphia, PA 19104
*Corresponding author email: hammer@seas.upenn.edu

Abstract.

Motility is critical for the function of T-lymphocytes. Motility in T-lymphocytes is driven by the occupancy of chemokine receptors by chemokines, and modulated by adhesive interactions. However, it is not well understood how the combination of adhesion and chemokine binding affects T-lymphocyte migration. We used microcontact printing on polymeric substrates to measure how lymphocyte migration is quantitatively controlled by adhesion and chemokine ligation. Focusing only on random motion, we found that T-lymphocytes exhibit biphasic motility in response to the substrate concentration of either ICAM-1 or VCAM-1, and generally display more active motion on ICAM-1 surfaces. Furthermore, we examined how the combination of the homeostatic chemokines CCL19 and CCL21 contribute to motility. By themselves, CCL19 and CCL21, ligands for CCR7, elicit biphasic motility, but their combination synergistically increases CCR7 mediated chemokinesis on ICAM-1. By presenting CCL21 with ICAM-1 on the surface with soluble CCL19, we observed random motion that is greater than what is observed with soluble chemokines alone. These data suggest that ICAM-1 has a greater contribution to motility than VCAM-1 and that both adhesive interactions and chemokine ligation work in concert to control T-lymphocyte motility.

Introduction

Recruitment of T lymphocytes (T cells) into lymphoid organs and peripheral tissues during immune surveillance and inflammation is critical for their function. T lymphocytes make use of the integrins Lymphocyte Function Associated Antigen-1 (LFA-1; αLβ2) and Very Late

Antigen-4 (VLA-4; α4β1) in cell trafficking, TCR formation and maturation, cell-to-cell binding, and motility within secondary lymphoid organs (SLOs) and tissues [1-4].

Within SLOs, T lymphocytes are exposed to adhesion ligands and chemokines that coordinate interactions between T lymphocytes and antigen presenting cells [5-8]. *In vivo* it is thought that in order for T lymphocytes to reach their destination, migrating cells must sense a gradient of soluble or surface immobilized chemokine(s) released from a distant source providing them with a chemotactic cue for directed migration [6, 9]. Within the SLO, homeostatic chemokines such as CCL19 and CCL21 are thought to play a key role in controlling migration and regulating the dynamics of motility by binding to the CCR7 receptor. It has been shown *in vitro* that T cells undergo chemotaxis in response to CCL19 and CCL21 within microfluidic devices [10]. However, the role that adhesion molecules play in regulating the response to chemokines is under appreciated.

Although it is commonly thought that directional migration in chemokine gradients is needed for lymphocyte positioning in the SLOs, it is possible that chemokinesis plays a strong role in lymphocyte exploration within the SLOs. There is no convincing evidence for directional trafficking of T lymphocytes under steady-state conditions as observed within explanted lymph nodes, but adhesive ligands and chemokines expressed by fibroblastic reticular cells have been shown to guide migration within the lymph nodes to facilitate T-lymphocyte activation [10-16]. It has been shown *in vivo* that T cells are capable of migrating at speeds up to 40 μm/min with frequent changes in direction [11]. At uniform concentrations, chemokines are capable of modulating cell speeds, and the observed random migration of T lymphocytes observed within lymph nodes may be due to a chemokinetic response to near-uniform levels of chemokines in the tissue [5, 17]. Additionally, binding of these chemokines to their G_i-protein-coupled receptor, CCR7, are capable of altering motility by modulating integrin activity through inside-out signaling pathways that indirectly modulate T cell homing to SLOs [5, 18, 19]. Recent work has elucidated the importance of the coordination of chemokines and adhesive ligands to support migration, but the exact interplay between the two is still not fully understood [5, 20-22].

Presentation of the ligands Intracellular Adhesion Molecule-1 (ICAM-1) and Vascular Cell Adhesion Molecule-1 (VCAM-1) to their corresponding cognate receptors LFA-1 and VLA-4 in the absence of chemokine is capable of inducing polarization critical for adhesion and motility via reorganization of the actin and microtubule cytoskeletons [19, 23-25]. Studies have

shown that CCL21 is capable of synergizing with adhesion ligands to increase adhesion, speed, and random motility *in vitro* [5]. However, to our knowledge, there has not been a quantitative analysis of the contributions of ICAM-1 and VCAM-1 on random motility in the absence of chemokines (haptokinesis) and the effect of varying chemokine concentrations (chemokinesis).

In this paper, we measured the motility of primary human T lymphocytes on different densities of the cell adhesion molecules ICAM-1 and VCAM-1 on microcontact printed PDMS substrates. This technology allows for the precise control of the density and type of adhesion molecule present on the surface; for example, we recently used microcontact printing to show how different densities of fibronectin can elicit a phenotypic switch in neutrophil motility [26]. Specifically, we investigated how the random motility of lymphocytes is controlled by varying concentrations of adhesion ligands, first in the absence and then in the presence of chemokine. We found that T lymphocytes exhibit biphasic motility when either ICAM-1 or VCAM-1 is presented alone in the absence of chemokine, with an overall greater motility on ICAM-1 substrates than VCAM-1. Then, we measured the effects of CCL19 and CCL21 on the motility of T lymphocytes and how combinations of the two chemokines modulate their motility. We found that individually, CCL19 and CCL21 also elicit similar biphasic motility with a peak in the random motility coefficient near an intermediate concentration of chemokine, and when combined, synergize to increase random motility. Furthermore, this synergistic effect is maintained when CCL21 is presented on the surface with soluble CCL19 on ICAM-1 surfaces. These results provide insight to how adhesive ligands and chemokines control the random migration of T lymphocytes in the absence of chemokine gradients.

Results and Discussion

Microcontact printing of Protein A/G and T lymphocyte adhesion

Protein A/G is a molecule produced through the fusion of the Fc-binding domains of Protein A and Protein G. Use of this molecule in conjunction with Fc-chimera ligands, such as ICAM-1/Fc and VCAM-1/Fc, has proven effective to immobilize chimeric proteins bearing the Fc domain [27]. We used microcontact printing of Protein A/G to prepare surfaces with controlled ratios of adhesion ligands linked to the Fc chimeras while keeping total protein concentration constant. This is achieved by varying the ratios of ICAM-1/Fc and VCAM-1/Fc molecules and human IgG_1. The steps for microcontact printing for our experimental system are illustrated in Supplemental Figure 1.

Primary human T lymphocytes do not polarize and migrate on microcontact printed Protein A/G alone or on Protein A/G surfaces incubated with human IgG_1 as indicated by a rounded morphology (Fig. 1A). Figure 1B demonstrates the fidelity of microcontact printing and the binding selectivity of primary human T lymphocytes to ICAM-1/Fc surfaces.

Either ICAM-1 and VCAM-1 alone trigger T lymphocyte haptokinesis

Primary human T lymphocytes adhere and migrate on PDMS surfaces printed with ICAM-1 and VCAM-1. We measured haptokinesis on these ligands by quantifying the mean-squared displacements over a range of ligand concentrations in the absence of chemokine. From the mean-squared displacements over time, we could determine the speed, persistence time, and random motility coefficient for each condition. T lymphocytes plated on ICAM-1 or VCAM-1 surfaces were tracked for 30 minutes. As illustrated by representative single-cell migration tracks (Fig. 2A, Movie S1, Movie S2, ESI†), T lymphocytes migrated substantial distances on both 0.5 and 5.0 μg/ml of ICAM-1 or VCAM-1 with no preferred direction. This remained true for all other concentrations of ligand tested (Data not shown). It is known that through LFA-1 ($\alpha_L\beta_2$) and VLA-4 ($\alpha_4\beta_1$) integrin interactions T lymphocytes are capable of migrating on ICAM-1 and VCAM-1 surfaces, respectively; we verified this through functional integrin blocking. Blocking of the α_L and β_2 integrin chains resulted in a significant decrease in cell adhesion on ICAM-1 relative to the positive control without antibody present ($p < 0.01$) (Fig. 2B). By targeting the β_1 integrin, a significant decrease in cell adhesion on VCAM-1 relative to the positive control without antibody present was observed ($p < 0.01$) (Fig. 2B). These data led us to attribute the observed ICAM-1 and VCAM-1-induced adhesion and resulting motility to the specific ligation of $\alpha_L\beta_2$ and $\alpha_4\beta_1$ with their cognate ligands on these microcontact printed surfaces.

Using the mean-squared displacements (MSD), we found that migrating T lymphocytes on ICAM-1 surfaces traveled greater distances than on VCAM-1 surfaces as suggested by larger MSDs with increasing time for both representative concentrations (Fig. 2C). This demonstrates that the dynamics of T lymphocyte motility on ICAM-1 and VCAM-1 are distinct. The use of random walk theories is common to quantify mammalian cell migration. The MSDs of migration can be scaled as $x^2(t) \propto t^{\alpha}$ during $0 < t < 90$ minutes where fitting can be used to determine the exponent α to classify the type of motion for each type and concentration of

ligand. Random or Brownian motion is observed for the value of $\alpha = 1$ and ballistic motion is observed for $\alpha = 2$, while values between the two are categorized as superdiffusive motion. Cells migrating on ICAM-1 surfaces display an average α over all concentrations of 1.48, indicating that T lymphocytes on ICAM-1 migrate superdiffusively through LFA-1 mediated interactions. Similarly on VCAM-1, T lymphocytes display superdiffusive motion with an average α of 1.21. This data is consistent with the recent observation that neither effector CD8+ T cells *in vivo* nor neutrophils on microcontact printed fibronectin PDMS surfaces display pure diffusive motion [26, 28].

To further characterize the motility of T cells on ICAM-1 and VCAM-1 surfaces, we used the experimental mean-squared displacements of each cell population with the persistent random walk model to fit for speed and persistence time. T lymphocytes were shown to have lager cell speeds on varying concentrations of ICAM-1 when compared to VCAM-1 (Fig. 2D; left graph); migrating T lymphocytes had average peak speeds (S) of 11.9 ± 1.12 μm/min and 4.3 ± 0.83 μm/min on 1.0 μg/ml of ICAM-1 and VCAM-1, respectively. These values correspond to observations of speed as seen previously *in vivo* and *in vitro* by other groups [9, 13, 14, 29, 30]. Persistence times (P) ranged from 1.9 ± 0.3 to 5.1 ± 0.7 minutes on ICAM-1 and 4.5 ± 0.7 to 8.9 ± 0.6 minutes on VCAM-1 (Fig. 2D; middle graph). In our system, higher cell speeds were observed on ICAM-1 compared to VCAM-1 ($S_{ICAM\text{-}1} > S_{VCAM\text{-}1}$) while generally cells were more persistent on VCAM-1 than ICAM-1 ($P_{ICAM\text{-}1} < P_{VCAM\text{-}1}$). Previous empirical observations have showed that speed and persistence times are inversely correlated across a variety of cells types with high speeds correlating to short persistence times and vice versa [31]. By plotting the speeds and persistence times across all concentrations of ICAM-1 and VCAM-1, we observed that this inverse correlation holds true for primary human T lymphocytes with a coefficient of determination (R^2) of 0.7699 (Fig. 2D; right graph). Overall, on ICAM-1 surfaces, T-lymphocytes have higher speeds with lower persistence times ($\uparrow S_{ICAM\text{-}1}$, $\downarrow P_{ICAM\text{-}1}$) and on VCAM-1 surfaces, T lymphocytes have lower speeds with higher persistence times ($\downarrow S_{VCAM\text{-}1}$, $\uparrow P_{VCAM\text{-}1}$). These data suggests that each ligand stimulates different adhesion signaling pathways.

The random motility coefficient (μ) is a metric that is commonly used to quantify migration in response to ligands or cytokines in a population of cells and is the product of the average cell speed (S) and mean-free path length (SP) divided by the dimensionality of the

system; therefore, it depends on the square of the speed and the first power of the persistence time. Figure 2E demonstrates that the random motility coefficient increases with increasing concentration of either ligand before reaching a maximum and then decreases; in other words, the behavior is biphasic. On ICAM-1, the highest random motility coefficient (μ_{ICAM-1}) is 160 μm^2/min, observed over a range of ICAM-1 concentrations between 0.5 to 10.0 μg/ml. T lymphocytes display a maximum μ_{VCAM-1} of 103 ± 16.1 μm^2/min at 0.5 μg/ml VCAM-1. The biphasic response of random motility with ligand density has been observed in other systems, and is often explained by the ratio of cell-substratum adhesiveness to cell contractility that would promote the highest level of motility [32-34]. Overall, we found that cells exhibit greater motility on ICAM-1 than VCAM-1 ($\mu_{ICAM-1} > \mu_{VCAM-1}$) for all concentrations tested.

Our data demonstrates that primary human T lymphocytes adhere and migrate differently on ICAM-1 and VCAM-1 microcontact printed PDMS substrates. It is known that T lymphocytes are capable of robust migration on ICAM-1 surfaces in the absence of chemokine predominantly driven by outside-in signaling triggering full LFA-1 activation [35, 36]. VLA-4, on the other hand, has been classically known to require chemokine engagement to achieve full integrin activation and induce cell polarization; this may explain why we observed decreased motility on VCAM-1. With this said, we observed competent T lymphocyte migration on VCAM-1 alone in the absence of chemokine which has not been observed by other laboratories [37].

Phenotypes of motility on the two ligands

Cell polarization and motility require the dynamic rearrangement of the actin and microtubule cytoskeletons through signaling pathways involving the Rho family GTPases [38-40]. Studies have also demonstrated that chemokines regulate integrin adhesive activity by modulating avidity and affinity and induce distinct polarized cell morphology [41-43]. In order to investigate the mechanisms of motility of T lymphocytes on ICAM-1 and VCAM-1, we plated cells on 5.0 μg/ml of either ICAM-1 or VCAM-1. We found no difference in cell area between ICAM-1 (189.6 ± 36.3 μm^2; n = 281) and VCAM-1 (173.4 ± 55.9 μm^2; n = 127), (Fig. 3A). After plating T lymphocytes on 5.0 μg/ml of ICAM-1 and VCAM-1, we fixed and permeabilized the cells, and fluorescently labeled their actin and microtubule cytoskeletons. Based upon our observations, we observed the following T lymphocyte phenotypes (Fig. 3C):

- Polarized, Motile – cells which migrated several cell diameters with a polarized morphology involving a clearly identifiable lamellipod, cell body, and uropod;
- Polarized, Tethered – lymphocytes with a polarized morphology but tethered and unable to move;
- Non-polarized, Motile – migrating several cell diameters with protrusions but lacking a clear polarized morphology;
- Non-polarized, Non-motile – spherical cells which do not have protrusions and are not migrating.

ICAM-1 surfaces induce increased lamellipod formation and greater cell adhesion when compared to VCAM-1 surfaces (Fig. 3B, left column). There are higher percentages of polarized and motile T lymphocytes on ICAM-1 than VCAM-1 surfaces (37% versus 12%; Fig. 3D and 3E). Also, ICAM-1 surfaces have fewer non-polarized and non-motile lymphocytes compared to VCAM-1 surfaces (23% versus 69%).

Effect of chemokines on T-lymphocyte motility

It is known that chemokines are capable of modulating T lymphocyte migration by promoting integrin activation and Rho GTPase signaling and synergize with adhesion ligands to alter adhesion, polarity, and motility [5]. The chemokine CCL21 is known to adhere to surfaces and affect leukocyte motion [22, 44, 45]. We investigated whether printing the chemokine CCL21 would increase the number of polarized and motile lymphocytes in tandem with either ICAM-1 or VCAM-1. We found that hCCL21 does not significantly change lamellipod formation of T lymphocytes on ICAM-1 ($n = 244$; Fig. 3B, top row) while it increases lamellipod formation on VCAM-1 surfaces ($n = 267$; Fig. 3B, bottom row). The fraction of polarized and motile lymphocytes on ICAM-1 with or without hCCL21 did not change (37% versus 40%; Fig. 3D). However, hCCL21 increased the fraction of polarized and migratory cells significantly on VCAM-1 surfaces (12% versus 22%) leading to a decrease in the percentage of non-polarized and non-motile cells (69% versus 52%; Fig. 3E) ($p < 0.05$).

Our data demonstrates that T lymphocytes are capable of spontaneous adhesion and migration to ICAM-1 and VCAM-1 surfaces in the absence of chemokine. We also

demonstrated that by the addition of CCL21 to the surface, T lymphocytes significantly increase cell polarity and migration on VCAM-1 but not on ICAM-1 surfaces.

CCL19 and CCL21 individually induce T lymphocyte chemokinesis that is dependent on ICAM-1 concentration

The chemokines CCL19 and CCL21 bind to the CCR7 receptor and are capable of driving chemokinesis and chemotaxis [46-49]. Previous studies have predominantly used transwell assays to demonstrate chemokinesis and chemotaxis, but these three dimensional assays provided limited ability to directly observe cells [20, 21, 50]. After having determined the effect of ligand composition and densities on the motility of primary human T lymphocytes, we investigated how soluble CCL19 (sCCL19) and CCL21 (sCCL21) drive CCR7-mediated chemokinesis on ICAM-1 microcontact printed PDMS surfaces and, specifically, how ligand concentration plays a role in the cell's ability to respond to chemokine concentration. We designated ICAM-1 concentrations of 5.0 μg/ml as *high* and 0.05 μg/ml as *low*; these two concentrations support spontaneous and robust T lymphocyte migration, as shown above. We measured the random motility coefficient for a range of CCL19 and CCL21 chemokine concentrations on both *high* and *low* concentrations of ICAM-1. We observed no significant differences in the random motility coefficients as a function of chemokine concentration on the *high* ICAM-1 surface with random motility coefficients (μ_{HIGH}) ranging between 164 ± 14.4 to 226 ± 40.6 μm^2/min (Fig. 4A). We have showed that T lymphocytes are capable of sustained motility on ICAM-1 alone without the need for chemokines, leading us to believe that sustained signaling through LFA-1/ICAM-1 interactions at this high ligand concentration was overwhelming the signals that resulted from CCR7 receptor engagement (outside-in versus inside-out signaling). On the *low* ICAM-1 surface, we observed a biphasic response in motility to chemokine concentrations. Statistically significant peaks in the random motility coefficients (μ_{LOW}) were observed at 20 nM for both sCCL19 (114.83 ± 4.76 μm^2/min) and sCCL21 (109.37 ± 8.77 μm^2/min) when compared to the random motility coefficient observed on *low* ICAM-1 alone ($p < 0.05$; Fig. 4A; Fig. S2). Empirical observations in other cell systems have estimated the K_D of the CCR7 receptor to be near 10 nM, which is close to the value of 20 nM that corresponds to our observed peaks in the random motility coefficients for both CCR7 ligands [51, 52]. Furthermore, Fig. 4B shows that T cell persistence times and speeds change with the addition of chemokines while still maintaining an

inverse correlation as seen in the absence of chemokine. Almost all chemokine concentrations led to decreased speeds with increased persistence times except at our maximum motility coefficient seen at sCCL21 and sCCL19 = 20 nM which had increased speeds and shorter persistence times (Fig. 4B; right panel).

Combinatorial chemokine signaling on ICAM-1 surfaces increases chemokinesis

We have demonstrated that varying ligand concentration (haptokinesis) and chemokine concentration (chemokinesis) can affect T lymphocyte motility. We next examined how T lymphocyte motility can be modulated by combining soluble CCL19 and CCL21 together, which both bind to the CCR7 receptor. Previous studies have shown that these ligands elicit different responses upon binding to CCR7 owing to receptor internalization and desensitization and signal attenuation [48, 53-55]. It has also been shown that murine dendritic cells and human T lymphocytes are capable of differential responses during chemotaxis to gradients of CCL19 and CCL21 [10, 52]. It is thought that within the lymph node, T lymphocytes encounter antigen presenting cells, such as dendritic cells, through random, autonomous motility within chemokine fields [11]. This led us to believe that by exposing primary human T lymphocytes to varying uniform fields of both sCCL19 and sCCL21, we would observe a difference in motility than what was seen with sCCL19 or sCCL21 alone. Interestingly, we found that the chemokines act together to increase motility greater than what was observed with the chemokines individually. A peak in motility was observed when T lymphocytes were exposed to 1 nM of both sCCL19 and sCCL21 with a random motility coefficient of 203.00 ± 11.45 μm^2/min (Fig. 5, Fig. S3B). For all equivalent concentrations of chemokines tested, the effect is superadditive producing random motility coefficients that are greater than the sum of the values observed individually with each chemokine except for the 20 nM condition. Our previous data has shown that for 100 nM and 200 nM of sCCL19 and sCCL21 individually, the motility coefficients are much lower than the maximum observed random motility coefficients found at 20 nM for each chemokine. Surprisingly, when 100 nM sCCL19 and 100 nM sCCL21 were combined, the random motility coefficient increased significantly implying a synergistic effect (172.87 ± 16.12 μm^2/min). Furthermore, this effect was also observed when 200 nM sCCL19 and 200 nM sCCL21 were combined (146.23 ± 36.45 μm^2/min). The combination of both 20 nM of sCCL19 and sCCL21 produced no significant changes in the motility coefficient when compared to that of the

chemokines individually, with a random motility coefficient of 129.28 ± 4.82 μm^2/min. We then tested the effects of combining a high concentration of one chemokine with another that is near the K_D of the receptor. For cells exposed to 20 nM of sCCL19 and 200 nM of sCCL21, we observed a random motility coefficient that is between what was observed on the two surfaces alone, 148.71 ± 12.41 μm^2/min. Furthermore, when we exposed cells to 200 nM of sCCL19 and 20 nM of sCCL21, we again observed an intermediate random motility coefficient equal to 114.30 ± 11.92 μm^2/min.

It is known that CCL19 and CCL21 elicit different responses upon CCR7 engagement, and the synergy we observed in our chemokinesis experiments in which we combined the two chemokines is likely a direct result of these different responses. The CCR7 receptor is recycled upon chemokine binding with CCL19 eliciting rapid internalization when compared to CCL21; furthermore, once internalized, CCL19 is targeted for degradation while CCL21 is not [53-55]. We suspect that larger quantities of free CCL21 is capable of binding to CCR7 since it is not targeted for degradation. This would lead to increased unbound CCR7 on the cell surface that can then be engaged to promote increased chemokinesis. These in vitro data provides further insight into how T lymphocytes respond to combinatorial chemokine signaling and the effect on their motility in conditions possibly similar to what is seen in SLOs through dual chemokine engagement.

Printed CCL21 and soluble CCL19 promote robust chemokinesis on ICAM-1 surfaces

We have demonstrated that soluble CCL19 and CCL21 can lead to combinatorial chemokine signaling with enhanced levels of motility. It is well understood that CCL21 is capable of triggering integrin-dependent adhesion of peripheral blood T lymphocytes under shear flow *in vitro*, and is displayed to flowing lymphocytes at the surface of high endothelial venules (HEVs) and within the T cell zones of the SLOs [56, 57]. CCL19, on the other hand, is not presented on a surface in large enough quantities but rather expressed in soluble form to act upon their common receptor, CCR7 [6, 58]. Furthermore, it is not well understood why two chemokine ligands capable of binding the same receptor are expressed in the same regions, but it can be thought that one, CCL21, promotes T lymphocyte binding to the HEVs while soluble CCL19, in concert with CCL21, is needed for recruitment of T lymphocytes to the T cell zones of the SLOs. To further understand the contribution of ligand presentation to T lymphocyte motility, we

performed chemokinesis experiments that mimic the expression pattern of these chemokines *in vitro* by exposing primary human T lymphocytes to microcontact printed CCL21 (hCCL21) along with varying concentrations of soluble CCL19 (sCCL19) on *low* ICAM-1 surfaces.

We observed with the addition of varying sCCL19 concentrations to ICAM-1 with hCCL21 there were no significant differences in speed with values ranging between 8.57 ± 0.55 to 10.27 ± 0.41 μm/min (Figure 4D; left panel). For persistence times, there was no significant differences with varying sCCL19 concentrations but a peak was observed at 100 nM with a P of 7.02 ± 2.43 minutes (Figure 4D; middle panel). This value is essentially half of what was observed at 100 nM sCCL19 on *low* ICAM-1 without hCCL21. The previous observed inverse correlation between speed and persistence time was lost with the addition of sCCL19 to hCCL21; the speed remains constant while persistence times shift (Figure 4D; right panel). However, these speeds do correlate to our previous observations at 20 nM of sCCL19 and sCCL21 alone.

The addition of hCCL21 to *low* ICAM-1 surfaces in the absence of sCCL19 more than doubles the random motility coefficient of cells compared to values observed on *low* ICAM-1 alone (195.55 ± 14.1 versus 83.37 ± 26.7 μm^2/min; Fig. S3C, Fig. S3D). When sCCL19 concentrations were varied, a peak in motility was observed at 100 nM of sCCL19 with a random motility coefficient value of 275.63 ± 31.3 μm^2/min (Figure 4E; $p < 0.05$). This is the largest random motility coefficient recorded in all sets of experiments indicating the importance of the difference in presentation patterns for CCL19 and CCL21. Due to CCL19 and CCL21 both being constitutively expressed by stromal cells within the T cell zones and CCL21 expressed by the HEVs, these data may represent what is seen physiologically and further indicates possible requirements for T lymphocyte recruitment.

By printing CCL21, we have shown that T lymphocytes are capable of robust migration on ICAM-1 with high speeds, and with the addition of 100 nM sCCL19, T lymphocytes have an increased persistence time which may assist in increased directional migration required for recruitment to the SLOs.

Conclusions

Here, we measured the migration of primary human T lymphocytes on ICAM-1 and VCAM-1 microcontact printed PDMS surfaces. Our results show that ligand composition and concentration are essential in controlling spontaneous and robust T lymphocyte motility by modulating their speed, persistence time, and thus their random motility. These haptokinesis studies also demonstrated that through non-Brownian motion T lymphocytes are more active on ICAM-1 than VCAM-1 surfaces. From chemokinesis studies on *low* ICAM-1 surfaces, we have demonstrated that chemokine signaling elicits biphasic motility with peaks in the random motility coefficient near the K_D of the CCR7 receptor for both CCL19 and CCL21 and is dependent on ligand concentration. By combining both soluble CCL19 and CCL21, T lymphocyte motility was increased to levels above what was observed by each chemokine individually through synergistic effects. We also demonstrated that by microcontact printing CCL21, we can double the motility of T lymphocytes on ICAM-1, and with the addition of soluble CCL19, we can further increase motility to levels that are higher than exposure to both soluble CCL19 and CCL21, combined or individually. These data provides insight into the dynamic behavior of T lymphocytes and the roles of ligand, chemokines, and combinatorial signaling in an effort for controlling motility to and within the SLOs. Furthermore, our finding that the motility of T-cells in not diffusive is consistent with measurements of made of the migration of murine CD8+ T lymphocytes *in vivo* which undergo Levy walks in response to CXCL10; this is believed to enhance the ability of T lymphocytes to encounter rare targets with more efficiency than Brownian motion walkers [28].

Our current work follows upon work from the Irvine laboratory on the motility of murine T lymphocytes on surfaces coated with ICAM-1, VCAM-1, and fibronectin. Consistent with what was shown here, the chemokine CCL21 enhanced motion, and that enhancement was dependent on the presence of an adhesive ligand. They did not, however, investigate the effects of printing hCCL21 on surfaces, quantify the random motility coefficient under any conditions, or identify the synergy of motility from two different chemokine molecules [5]. As we previously showed with neutrophils, our ability to print molecules on substrates allows us to identify modes of motility that cannot be observed on traditional surfaces [26]. We look forward to using this powerful tool to further examine mechanisms of motility of immune cells in the future.

Acknowledgements

We are grateful to Eric Johnston for technical assistance in the laboratory. Funding for this work was provided by NIH AI082292.

Figure captions.

Fig. 1 T lymphocytes adhere to microcontact printed PDMS substrates. (A) Phase contrast images showing rounded morphologies for T lymphocytes indicating no polarity and adhesion to Protein A/G or human IgG1 alone. Scale bars, 100 μm (B) Phase contrast, fluorescence, and overlay images showing the fidelity of microcontact printed protein A/G-Alex Fluor 555 conjugate on PDMS surfaces and binding selectivity of T lymphocytes to ICAM-1/Fc. Scale bars, 100 μm.

Fig. 2 T lymphocytes are more migratory on ICAM-1 than VCAM-1. (A) Representative single-cell migration tracks for T lymphocytes on 0.5 and 5.0 μg/ml of ICAM-1 and VCAM-1 showing no preferred direction. (B) Antibody blocking against αLβ2 and β1 integrins show decreased cell adhesion to ICAM-1 and VCAM-1 substrates, respectively; *$p < 0.05$, compared to isotype; one-sample t test. (C) MSD versus time showing linear trends for different concentrations of ICAM-1 and VCAM-1. MSD can be scaled as $x^2(t) \propto t^{\alpha}$ indicating that T lymphocytes acquire displacement superdiffusively ($\alpha > 1$). Numbers on line represent approximate values of α. (D) T lymphocyte speeds and persistence times determined from using the persistent random walk model (left two graphs); cells have faster speeds and shorter persistence times on ICAM-1 with lower speeds and longer persistence times on VCAM-1. The right graph shows that across all concentrations of ligand an inverse correlation is maintained between persistence time and cell speed. (E) Comparison of the random motility coefficients (μ) show biphasic motility as a function of ligand concentration with ICAM-1 (peak μ_{ICAM-1} = 172.77 ± 45.45 μm^2/min) promoting increased haptokinesis than VCAM-1 (peak μ_{VCAM-1} = 103.58 ± 16.06 μm^2/min). The error bars represent the standard error of the mean (s.e.m.)

Fig 3. T lymphocytes are more polarized on ICAM-1 than VCAM-1. (A) Measurements found no difference in cell area for ICAM-1 (189.6 ± 36.3 μm^2; n = 281) versus VCAM-1 (173.4 ± 55.9 μm^2; n = 127) (B) Fluorescence images showing T lymphocytes on either ICAM-1 or VCAM-1 with or without hCCL21 on the surface. T lymphocytes visibly exhibit greater polarity (lamellipod, cell body, and uropod) on ICAM-1 surfaces with or without hCCL21 (top row) than compared to VCAM-1 surfaces (bottom row). Cells were stained with Alexa568 phalloidin (red) and Alexa488 anti-α-tubulin antibody (green). Scale bars, 10 μm. (C) Phase contrast and fluorescence images of the four classifications for T lymphocyte migration: polarized and motile, polarized and tethered, non-polarized and motile, and non-polarized and non-motile. (D) T lymphocytes were classified based upon their migratory phenotype on ICAM-1 (n = 281) with or without hCCL21. Around 37% of cells plated exhibited a polarized, motile phenotype. There was no observable differences with the addition of hCCL21 (n = 127). (E) On VCAM-1 (n = 244) surfaces, cells are less polarized and motile (12% of cells) and the addition of hCCL21 (n = 267 for VCAM-1) increases the number of polarized, motile lymphocytes while decreasing the number of non-polarized, non-motile cells on VCAM-1; *p < 0.05, compared to no CCL21; one-sample t test

Fig. 4. sCCL19 and sCCL21 individually induce chemokinesis on *low* ICAM-1 surfaces. (A) Comparison of the random motility coefficients (μ) for sCCL19 and sCCL21 show biphasic motility on *low* but not *high* ICAM-1 surfaces. Peak in chemokinesis observed at 20 nM (μ_{CCL19} = 174.13 ± 4.76 μm^2/min and μ_{CCL21} = 146.52 ± 8.77 μm^2/min); *p < 0.05, compared to all concentrations; one-sample t test. (B) T lymphocyte speeds and persistence times during chemokinesis for sCCL19 and sCCL21 (left two panels); cells maintain near same speeds and persistence times for each concentration of chemokine. The right graph shows that across all concentrations of chemokine an inverse correlation is maintained between persistence time and cell speed with an increased speed and decreased persistence time for 20 nM. The error bars represent the standard error of the mean (s.e.m.)

Fig. 5. sCCL19 and sCCL21 synergize for combinatorial chemokinesis on *low* ICAM-1 surfaces. Combined chemokinesis of sCCL19 and sCCL21 show that motility is increased to

levels greater than what is observed with each chemokine individually. Peak in chemokinesis observed at 1 nM sCCL19 and sCCL21 ($\mu = 203.00 \pm 11.45$ μm^2/min).

Fig. 6 hCCL21 and sCCL19 induce chemokinesis on *low* ICAM-1 surfaces. (A) T lymphocyte speeds and persistence times on 20 nM hCCL21 and varying sCCL19 concentrations (left two panels); speed remains constant with a peak in persistence time at 100 nM sCCL19. The right graph indicates a loss of the inverse correlation between speed and persistence time. (B) Peak in hCCL21 and sCL19 chemokinesis at 100 nM sCCL19 with the highest observed $\mu = 275.63 \pm 31.3$ μm^2/min; *$p < 0.05$, compared to no CCL21; one-sample t test The error bars represent the standard error of the mean (s.e.m.)

Supplemental Fig1. Microcontact printing of PDMS substrates. Illustration for microcontact printing of protein A/G followed by subsequent binding of either ICAM-1/Fc or VCAM-1/Fc with IgG_1.

Supplemental Fig2. CCL19 and CCL21 Chemokinesis. Single cell migration tracks showing random motility at (A) 20 nM CCL19 and (B) 20 nM CCL21 with no preferred direction in migration

Supplemental Fig3. Single cell tracks for combinatorial chemokinesis. Single cell migration tracks showing random motility on (A) 0.05 μg/ml of ICAM-1 alone (B) 1nM soluble CCL19 and 1 nM soluble CCL21 (C) 20 nM of printed CCL21 and (D) 20 nM of printed CCL21 with 100 nM soluble CCL19 with no preferred direction in migration

Movie1. Primary human T lymphocytes migrating on 5.0 μg/ml of ICAM-1. 20X, Scale bar = 50 μm

Movie 2. Primary human T lymphocytes migrating on 5.0 μg/ml of VCAM-1. 20X, Scale bar = 50 μm

Experimental

Cell culture and reagents

Human blood was obtained via venipuncture from healthy adult donors and collected into sterile tubes containing sodium heparin (BD Biosciences, San Jose, CA). Samples were collected with University of Pennsylvania Institutional Review Board approval from consenting adult volunteers. Blood samples were carefully layered in a 1:1 ratio of whole blood to 1-Step™ Polymorphprep (Axis-Shield, Oslo, Norway). Vials were then centrifuged at 1500 rpm for 35 minutes and the mononuclear band was collected into a fresh vial. Cells were cultured in RPMI-1640 supplemented with 10% FBS and 1 μg/ml of phytohemagglutinin (PHA-M; Sigma-Aldrich, St. Louis, MO) overnight. After 24 hours, the lymphocyte suspension in the PHA medium was transferred into a new flask leaving behind adherent cells. After an additional 48 hours, the cells were then cultured in RPMI-1640 with 10% FBS and 1% penicillin-streptomycin supplemented with 20 ng/ml of interleukin-2 (IL-2; Roche, Mannheim, Germany). Cells were used for experimentation following an additional 72 hours in culture. Other biological reagents included: protein A/G (Thermo Scientific, Rockford, IL), human ICAM-1/Fc and VCAM-1/Fc (R&D Systems, Minneapolis, MN), human IgG1 (Abcam, Kendall Square, MA), human anti-alphaL and human anti-beta2 (Calbiochem, San Diego, CA), human anti-alphaM (Millipore, Temecula, CA), human anti-beta1 (BD Pharmingen, San Jose, CA), CCL19/CCL21 (PreproTech, Rocky Hill, NJ), Pluronics F127 (Sigma-Aldrich, St. Louis, MO), Alexa568-labeled phalloidin and Alexa488-labeled mouse anti-α tubulin (Invitrogen, Grand Island, NY).

Substrate preparation

Poly(dimethylsiloxane) (PDMS) (Sylgard 184 Silicone Elastomer, Dow Corning, Midland, MI) coated coverslips were prepared from number one thickness glass coverslips (Fisher Scientific, Hampton, NH) of 25 mm diameter spin coated with degassed PDMS (10:1 base:cure by weight) and cured overnight at 65 ºC. PDMS-coated coverslips were affixed to the bottom of six-well tissue culture plates which has been laser-cut to generate a 22 mm diameter opening in the bottom of the wells. Coverslip bonding was performed using a small amount of PDMS (10:1 base:cure by weight) and baked at 65 ºC for 30 minutes for curing.

Protein printing and blocking

Flat stamps for printing were prepared by pouring degassed PDMS mixed at 10:1 base:cure by weight over an unpatterned silicon wafer. The polymer was cured for 2 hours or longer at 65 ºC. Stamps were trimmed, sonicated in 200 proof ethanol for 10 minutes, rinsed with dH_2O, and dried in a stream of N_2(g). For motility studies, stamps were 1 cm^2 and were inked with 200 µl of 2 µg/ml of protein A/G in PBS for 2 hours at room temperature. The stamps were then thoroughly rinsed in H_2O and blown dry with a stream of N2. In parallel, the six-well PDMS coverslip substrate was treated with ultraviolet ozone for 7 minutes (UVO Cleaner Model 342, Jelight Company, Irvine, CA) to render the surface hydrophilic. The stamp was then placed in conformal contact with the substrate for ~10 seconds and removed. A 0.2% (w/v) solution of Pluronics F127 was immediately adsorbed to the PDMS substrates for 30 minutes at room temperature to prevent protein adsorption to non-functionalized portions of the PDMS. The cell culture substrate was then rinsed with PBS 3X without dewetting the functionalized surface before deposition of 200 µl of either ICAM-1/Fc or VCAM-1/Fc in PBS for 2 hours at room temperature. The surfaces were then rinsed with PBS 3X without dewetting before incubation with cells.

Haptokinesis and chemokinesis assay

PDMS substrates were prepared as described above. For printed CCL21 studies, 20 nM of CCL21 was inked with Protein A/G followed by stamping onto PDMS substrates. Before use, all substrates were washed 3X with phosphate-buffered saline. Each well was plated at 5 x 10^5 cells/ml in serum-free RPMI-1640 supplemented with 0.1% BSA and 2 mg/ml glucose. The substrate was then placed in a 37°C humidified atmosphere containing 5% CO_2 in air incubator for 15 minutes to allow for cell attachment. The wells were then gently washed 3X with PBS to remove non-adherent cells followed by imaging in a 5% CO_2 and 37°C environment for at least 1 hour. Cells were placed into a motorized stage and observed using a Nikon Eclipse TE_{300} phase contrast microscope. A 10X objective and 10X eyepiece were used for a final magnification of 100X. For chemokinesis assays, a CCL19 and/or CCL21 chemokine solution was dispensed into each well before imaging and performed on ICAM-1 substrates at a concentration of 0.05 µg/ml. For surface presentation of CCL21, stamps were inked with 2 µg/ml of Protein A/G and 250 ng/ml of CCL21 and printed onto the PDMS substrates before blocking and application of the Fc protein solution.

Measurement of cell trajectories and mean-squared displacements

Cell movement was tracked using the ImageJ plugin Manual Tracking. ImageJ and the plugin are both freely available through the NIH website (http://rsbweb.nih.gov/ij/). The centroid of the cell was considered to represent the cell position. Time lapse microscopy was used and images were taken every 1.5 minutes. The result was a series of (x,y) positions with time for each cell. The net displacement during the ith 1.5 minute increment, D_i, was calculated by the difference of the position at the beginning and end of that time step. The mean-squared displacement, $\langle D^2(t) \rangle$, over time was calculated using the method of non-overlapping intervals [59]. Speed, S, can be considered as the total path length over time and persistence time, P, is the time a cell remains moving without changing direction. S and P were obtained by fitting these to the persistent random walk equation (Dunn, 1983 $\langle D^2(t) \rangle = 2S^2\left[t - P\left(1 - e^{-t/P}\right)\right]$ where t is the time interval, using a non-linear least squares regression analysis [60, 61]. The mean-free path length (P_L) and random motility coefficient (μ) are then calculated as $P_L = PS$ and $\mu = \frac{1}{2}S^2P$ [62, 63].

Immunofluorescence

Primary human T lymphocytes were plated on 5.0 μg/ml ICAM-1/Fc and VCAM-1/Fc surfaces with or without 250 ng/ml of stamped CCL21 at 5 x 10^5 cells/ml for 1 h in a 37°C humidified atmosphere containing 5% CO_2. The cells were then fixed with 4% paraformaldehyde in PBS for 7 minutes. Cells were permeabilized with 0.2% Triton X-100 for 5 minutes and blocked with 1% BSA in PBS for 30 minutes at room temperature. Cells were incubated with 1:200 Alexa568-labeled phalloidin and Alexa488-labeled mouse anti-α tubulin (Invitrogen) for 30 minutes at room temperature. Cells were mounted in Fluoromount-G mounting medium (SouthernBiotech, Birmingham, Alabama) and examined by confocal microscopy (Leica SP5).

References

1. T. A. Springer, *Cell*, 1994, 76, 301-314.
2. E. C. Butcher and L. J. Picker, *Science*, 1996, 272, 60-66.

3. U. H. von Andrian and C. R. Mackay, *The New England journal of medicine*, 2000, 343, 1020-1034.
4. D. M. Rose, J. Han and M. H. Ginsberg, *Immunological reviews*, 2002, 186, 118-124.
5. A. N. Stachowiak, Y. Wang, Y. C. Huang and D. J. Irvine, *Journal of immunology*, 2006, 177, 2340-2348.
6. J. G. Cyster, *Annual Review of Immunology*, 2005, 23, 127-159.
7. R. Forster, A. C. Davalos-Misslitz and A. Rot, *Nature reviews. Immunology*, 2008, 8, 362-371.
8. A. Kaiser, E. Donnadieu, J. P. Abastado, A. Trautmann and A. Nardin, *Journal of immunology*, 2005, 175, 2349-2356.
9. C. Sumen, T. R. Mempel, I. B. Mazo and U. H. von Andrian, *Immunity*, 2004, 21, 315-329.
10. F. Lin and E. C. Butcher, *Lab on a chip*, 2006, 6, 1462-1469.
11. M. J. Miller, S. H. Wei, M. D. Cahalan and I. Parker, *Proceedings of the National Academy of Sciences of the United States of America*, 2003, 100, 2604-2609.
12. M. J. Miller, A. S. Hejazi, S. H. Wei, M. D. Cahalan and I. Parker, *Proceedings of the National Academy of Sciences of the United States of America*, 2004, 101, 998-1003.
13. P. Bousso and E. A. Robey, *Immunity*, 2004, 21, 349-355.
14. M. J. Miller, S. H. Wei, I. Parker and M. D. Cahalan, *Science*, 2002, 296, 1869-1873.
15. S. Nandagopal, D. Wu and F. Lin, *PloS one*, 2011, 6, e18183.
16. M. Bajenoff, J. G. Egen, L. Y. Koo, J. P. Laugier, F. Brau, N. Glaichenhaus and R. N. Germain, *Immunity*, 2006, 25, 989-1001.
17. S. A. Luther, A. Bidgol, D. C. Hargreaves, A. Schmidt, Y. Xu, J. Paniyadi, M. Matloubian and J. G. Cyster, *The Journal of Immunology*, 2002, 169, 424-433.
18. M. Shimonaka, K. Katagiri, T. Nakayama, N. Fujita, T. Tsuruo, O. Yoshie and T. Kinashi, *The Journal of cell biology*, 2003, 161, 417-427.
19. Y.-M. Hyun, C. Lefort and M. Kim, *Immunologic Research*, 2009, 45, 195-208.
20. R. Yoshida, M. Nagira, T. Imai, M. Baba, S. Takagi, Y. Tabira, J. Akagi, H. Nomiyama and O. Yoshie, *International immunology*, 1998, 10, 901-910.
21. J. J. Campbell, E. P. Bowman, K. Murphy, K. R. Youngman, M. A. Siani, D. A. Thompson, L. Wu, A. Zlotnik and E. C. Butcher, *The Journal of cell biology*, 1998, 141, 1053-1059.
22. E. Woolf, I. Grigorova, A. Sagiv, V. Grabovsky, S. W. Feigelson, Z. Shulman, T. Hartmann, M. Sixt, J. G. Cyster and R. Alon, *Nature immunology*, 2007, 8, 1076-1085.
23. A. D. Luster, R. Alon and U. H. von Andrian, *Nature immunology*, 2005, 6, 1182-1190.
24. M. P. Valignat, O. Theodoly, A. Gucciardi, N. Hogg and A. C. Lellouch, *Biophysical journal*, 2013, 104, 322-331.
25. G. Cinamon, V. Shinder and R. Alon, *Nature immunology*, 2001, 2, 515-522.
26. S. J. Henry, J. C. Crocker and D. A. Hammer, *Integrative Biology*, 2014, 6, 348-356.
27. M. Eliasson, A. Olsson, E. Palmcrantz, K. Wiberg, M. Inganäs, B. Guss, M. Lindberg and M. Uhlén, *Journal of Biological Chemistry*, 1988, 263, 4323-4327.
28. T. H. Harris, E. J. Banigan, D. A. Christian, C. Konradt, E. D. Tait Wojno, K. Norose, E. H. Wilson, B. John, W. Weninger, A. D. Luster, A. J. Liu and C. A. Hunter, *Nature*, 2012, 486, 545-548.
29. S. H. Wei, I. Parker, M. J. Miller and M. D. Cahalan, *Immunological reviews*, 2003, 195, 136-159.

30. L. Svensson, A. McDowall, K. M. Giles, P. Stanley, S. Feske and N. Hogg, *PloS one*, 2010, 5, e15090.
31. D. A. Lauffenburger and J. J. Linderman, *Receptors: Modeling for Binding, Trafficking, and Signaling*, Oxford University Press, New York, 1996.
32. S. P. Palecek, Loftus, J.C., Ginsberg, M.H., Lauffenburger, D.A., and A.F. Horwitz, *Nature*, 1997, 385, 537-540.
33. P. A. DiMilla, K. Barbee and D. A. Lauffenburger, *Biophysical journal*, 1991, 60, 15-37.
34. P. A. DiMilla, J. A. Stone, J. A. Quinn, S. M. Albelda and D. A. Lauffenburger, *The Journal of cell biology*, 1993, 122, 729-737.
35. A. Smith, M. Bracke, B. Leitinger, J. C. Porter and N. Hogg, *Journal of cell science*, 2003, 116, 3123-3133.
36. R. Evans, A. C. Lellouch, L. Svensson, A. McDowall and N. Hogg, *Blood*, 2011, 117, 3331-3342.
37. Y. M. Hyun, H. L. Chung, J. L. McGrath, R. E. Waugh and M. Kim, *Journal of immunology*, 2009, 183, 359-369.
38. T. Wittmann and C. M. Waterman-Storer, *Journal of cell science*, 2001, 114, 3795-3803.
39. A. J. Ridley, M. A. Schwartz, K. Burridge, R. A. Firtel, M. H. Ginsberg, G. Borisy, J. T. Parsons and A. R. Horwitz, *Science*, 2003, 302, 1704-1709.
40. M. Raftopoulou and A. Hall, *Developmental biology*, 2004, 265, 23-32.
41. Y. van Kooyk and C. G. Figdor, *Current opinion in cell biology*, 2000, 12, 542-547.
42. G. Constantin, M. Majeed, C. Giagulli, L. Piccio, J. Y. Kim, E. C. Butcher and C. Laudanna, *Immunity*, 2000, 13, 759-769.
43. M. A. del Pozo, P. Sánchez-Mateos, M. Nieto and F. Sánchez-Madrid, *The Journal of cell biology*, 1995, 131, 495-508.
44. M. Weber, R. Hauschild, J. Schwarz, C. Moussion, I. de Vries, D. F. Legler, S. A. Luther, T. Bollenbach and M. Sixt, *Science*, 2013, 339, 328-332.
45. K. Schumann, T. Lämmermann, M. Bruckner, D. F. Legler, J. Polleux, J. P. Spatz, G. Schuler, R. Förster, M. B. Lutz, L. Sorokin and M. Sixt, *Immunity*, 2010, 32, 703-713.
46. T. Worbs, T. R. Mempel, J. Bolter, U. H. von Andrian and R. Forster, *The Journal of experimental medicine*, 2007, 204, 489-495.
47. T. Okada and J. G. Cyster, *Journal of immunology*, 2007, 178, 2973-2978.
48. M. R. Britschgi, A. Link, T. K. Lissandrin and S. A. Luther, *Journal of immunology*, 2008, 181, 7681-7688.
49. R. Forster, A. Schubel, D. Breitfeld, E. Kremmer, I. Renner-Muller, E. Wolf and M. Lipp, *Cell*, 1999, 99, 23-33.
50. E. K. Frow, J. Reckless and D. J. Grainger, *Medicinal Research Reviews*, 2004, 24, 276-298.
51. R. Yoshida, M. Nagira, M. Kitaura, N. Imagawa, T. Imai and O. Yoshie, *Journal of Biological Chemistry*, 1998, 273, 7118-7122.
52. B. G. Ricart, B. John, D. Lee, C. A. Hunter and D. A. Hammer, *Journal of immunology*, 2011, 186, 53-61.
53. G. Bardi, M. Lipp, M. Baggiolini and P. Loetscher, *European journal of immunology*, 2001, 31, 3291-3297.
54. M. A. Byers, P. A. Calloway, L. Shannon, H. D. Cunningham, S. Smith, F. Li, B. C. Fassold and C. M. Vines, *Journal of immunology*, 2008, 181, 4723-4732.
55. C. Otero, M. Groettrup and D. F. Legler, *Journal of immunology*, 2006, 177, 2314-2323.

56. J. V. Stein, S. F. Soriano, C. M'Rini, C. Nombela-Arrieta, G. G. de Buitrago, J. M. Rodriguez-Frade, M. Mellado, J. P. Girard and A. C. Martinez, *Blood*, 2003, 101, 38-44.
57. R. A. Warnock, J. J. Campbell, M. E. Dorf, A. Matsuzawa, L. M. McEvoy and E. C. Butcher, *The Journal of experimental medicine*, 2000, 191, 77-88.
58. V. N. Ngo, H. Lucy Tang and J. G. Cyster, *The Journal of experimental medicine*, 1998, 188, 181-191.
59. R. B. Dickinson and R. T. Tranquillo, *Journal of Mathematical Biology*, 1993, 31, 7.
60. H. G. Othmer, S. R. Dunbar and W. Alt, *Journal of Mathematical Biology*, 1988, 26, 263.
61. G. A. Dunn, *Agents and Actions Supplements*, 1983, 12, 19.
62. C. L. Stokes, D. A. Lauffenburger and S. K. Williams, *Journal of cell science*, 1991, 99 (Pt 2), 419-430.
63. R. M. Ford and D. A. Lauffenburger, *Biotechnology and Bioengineering*, 1991, 37, 661-672.

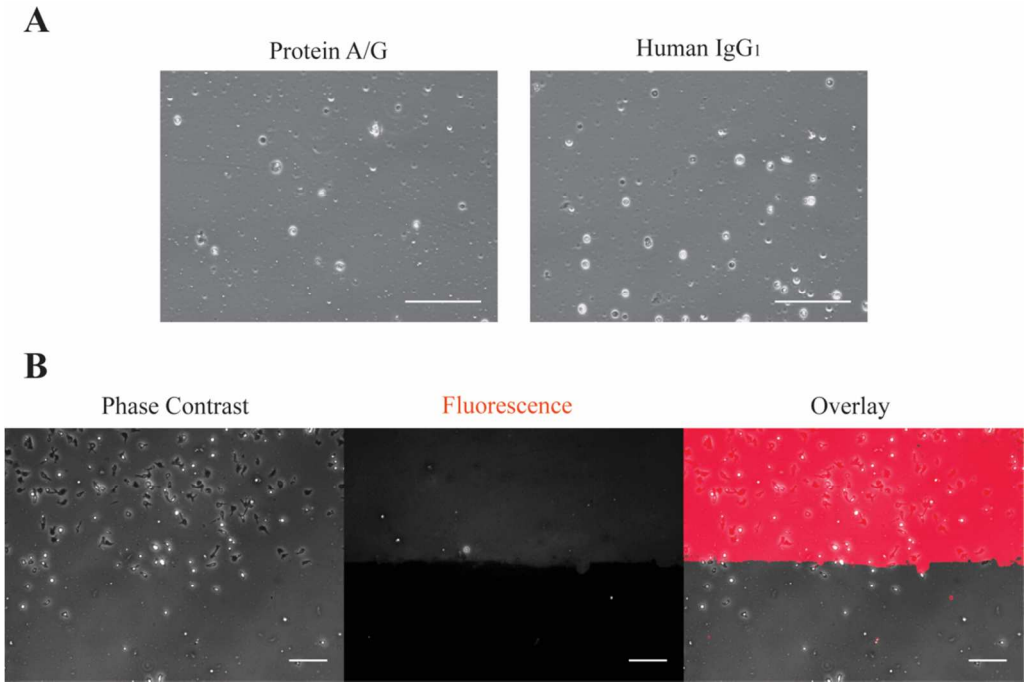

Fig. 1 T lymphocytes adhere to microcontact printed PDMS substrates. (A) Phase contrast images showing rounded morphologies for T lymphocytes indicating no polarity and adhesion to Protein A/G or human IgG1 alone. Scale bars, 100 µm (B) Phase contrast, fluorescence, and overlay images showing the fidelity of microcontact printed protein A/G-Alex Fluor 555 conjugate on PDMS surfaces and binding selectivity of T lymphocytes to ICAM-1/Fc. Scale bars, 100 µm.

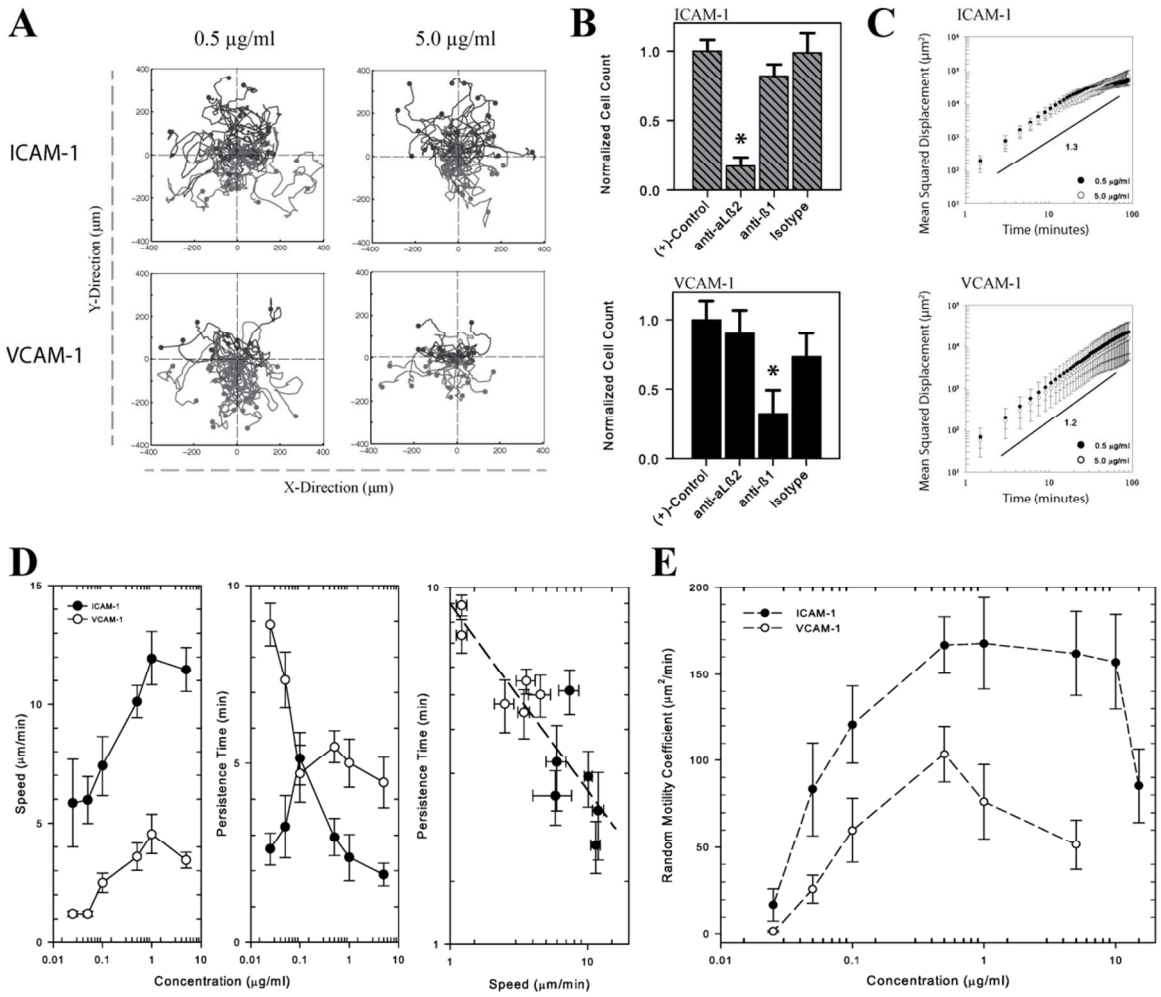

Fig. 2 T lymphocytes are more migratory on ICAM-1 than VCAM-1. (A) Representative single-cell migration tracks for T lymphocytes on 0.5 and 5.0 µg/ml of ICAM-1 and VCAM-1 showing no preferred direction. (B) Antibody blocking against $\alpha_L\beta_2$ and β_1 integrins show decreased cell adhesion to ICAM-1 and VCAM-1 substrates, respectively; *$p < 0.05$, compared to isotype; one-sample t test. (C) MSD versus time showing linear trends for different concentrations of ICAM-1 and VCAM-1. MSD can be scaled as $x^2(t) \propto t^{\alpha}$ indicating that T lymphocytes acquire displacement superdiffusively ($\alpha > 1$). Numbers on line represent approximate values of α. (D) T lymphocyte speeds and persistence times determined from using the persistent random walk model (left two graphs); cells have faster speeds and shorter persistence times on ICAM-1 with lower speeds and longer persistence times on VCAM-1. The right graph shows that across all concentrations of ligand an inverse correlation is maintained between persistence time and cell speed. (E) Comparison of the random motility coefficients (µ) show biphasic motility as a function of ligand concentration with ICAM-1 (peak $\mu_{ICAM\text{-}1}$ = 172.77 ± 45.45 µm^2/min) promoting increased haptokinesis than VCAM-1 (peak $\mu_{VCAM\text{-}1}$ = 103.58 ± 16.06 µm^2/min). The error bars represent the standard error of the mean (s.e.m.)

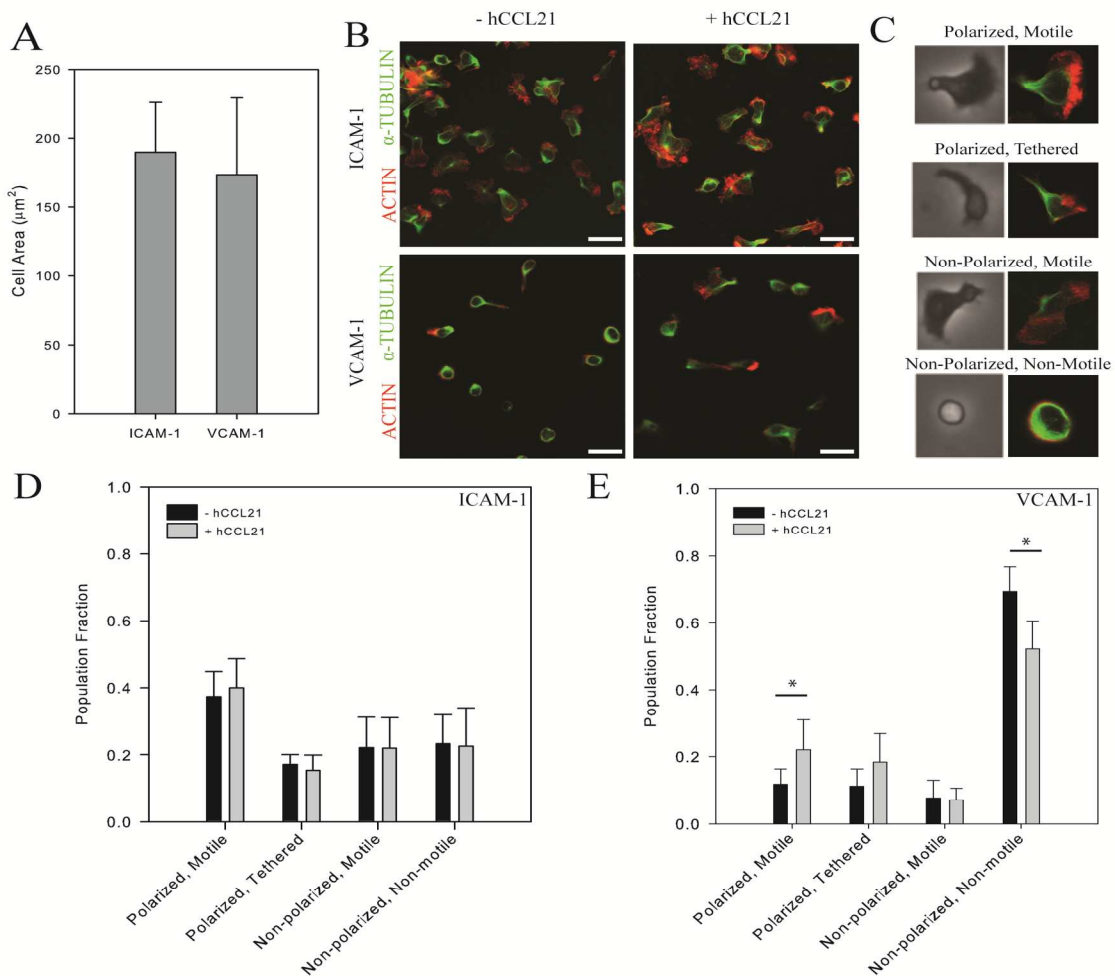

Fig 3. T lymphocytes are more polarized on ICAM-1 than VCAM-1. (A) Measurements found no difference in cell area for ICAM-1 (189.6 ± 36.3 μm^2; n = 281) versus VCAM-1 (173.4 ± 55.9 μm^2; n = 127) (B) Fluorescence images showing T lymphocytes on either ICAM-1 or VCAM-1 with or without hCCL21 on the surface. T lymphocytes visibly exhibit greater polarity (lamellipod, cell body, and uropod) on ICAM-1 surfaces with or without hCCL21 (top row) than compared to VCAM-1 surfaces (bottom row). Cells were stained with Alexa568 phalloidin (red) and Alexa488 anti-α-tubulin antibody (green). Scale bars, 10 μm. (C) Phase contrast and fluorescence images of the four classifications for T lymphocyte migration: polarized and motile, polarized and tethered, non-polarized and motile, and non-polarized and non-motile. (D) T lymphocytes were classified based upon their migratory phenotype on ICAM-1 (n = 281) with or without hCCL21. Around 37% of cells plated exhibited a polarized, motile phenotype. There was no observable differences with the addition of hCCL21 (n = 127). (E) On VCAM-1 (n = 244) surfaces, cells are less polarized and motile (12% of cells) and the addition of hCCL21 (n = 267 for VCAM-1) increases the number of polarized, motile lymphocytes while decreasing the number of non-polarized, non-motile cells on VCAM-1; *$p < 0.05$, compared to no CCL21; one-sample t test

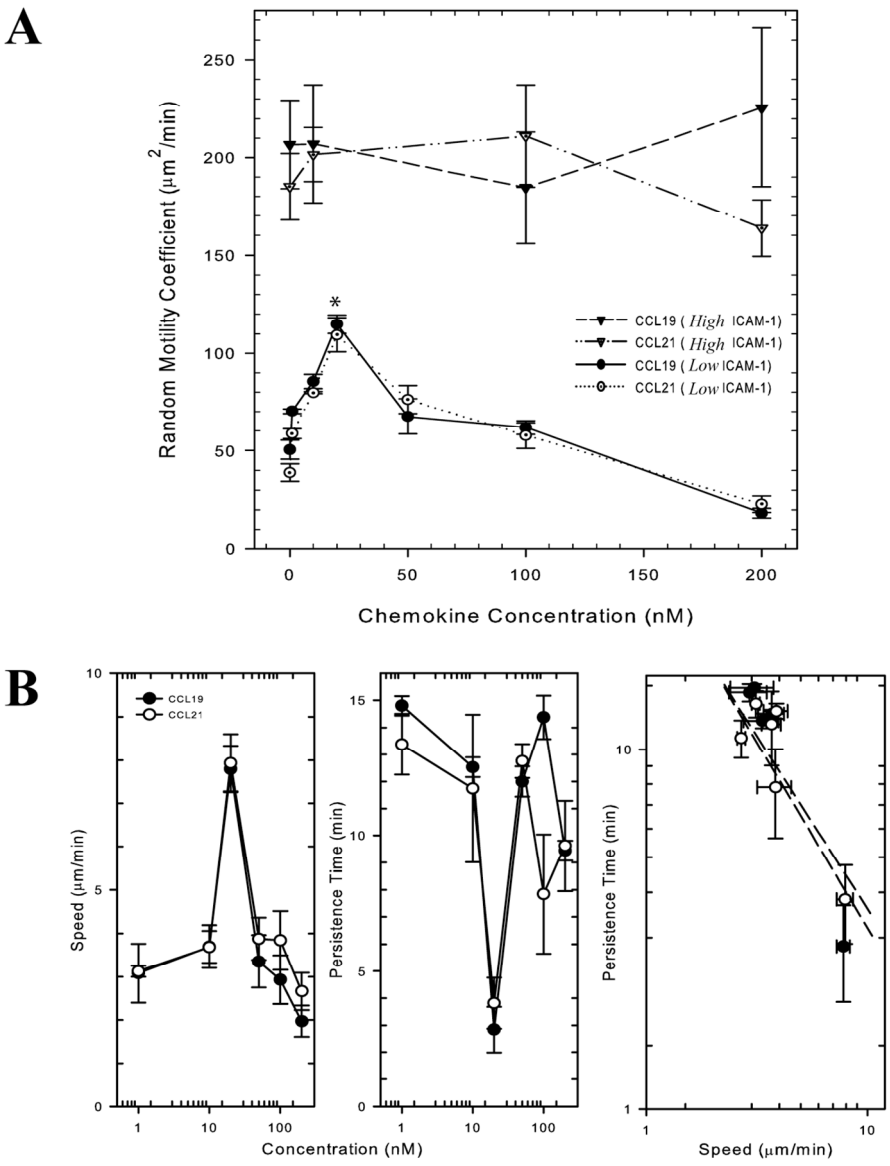

Fig. 4. sCCL19 and sCCL21 individually induce chemokinesis on *low* ICAM-1 surfaces. (A) Comparison of the random motility coefficients (μ) for sCCL19 and sCCL21 show biphasic motility on *low* but not *high* ICAM-1 surfaces. Peak in chemokinesis observed at 20 nM (μ_{CCL19} = 174.13 ± 4.76 μm²/min and μ_{CCL21} = 146.52 ± 8.77 μm²/min); *$p < 0.05$, compared to all concentrations; one-sample t test. (B) T lymphocyte speeds and persistence times during chemokinesis for sCCL19 and sCCL21 (left two panels); cells maintain near same speeds and persistence times for each concentration of chemokine. The right graph shows that across all concentrations of chemokine an inverse correlation is maintained between persistence time and cell speed with an increased speed and decreased persistence time for 20 nM. The error bars represent the standard error of the mean (s.e.m.)

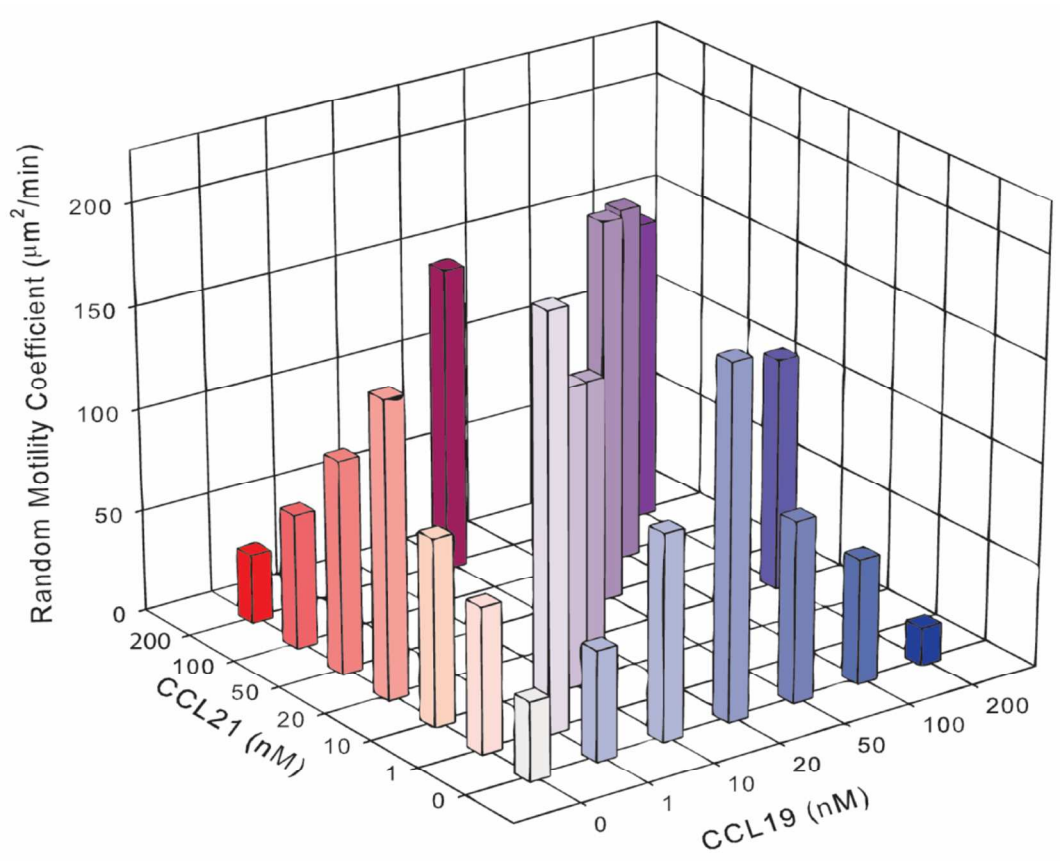

Fig. 5. sCCL19 and sCCL21 synergize for combinatorial chemokinesis on *low* ICAM-1 surfaces. Combined chemokinesis of sCCL19 and sCCL21 show that motility is increased to levels greater than what is observed with each chemokine individually. Peak in chemokinesis observed at 1 nM sCCL19 and sCCL21 ($\mu = 203.00 \pm 11.45$ $\mu m^2/min$).

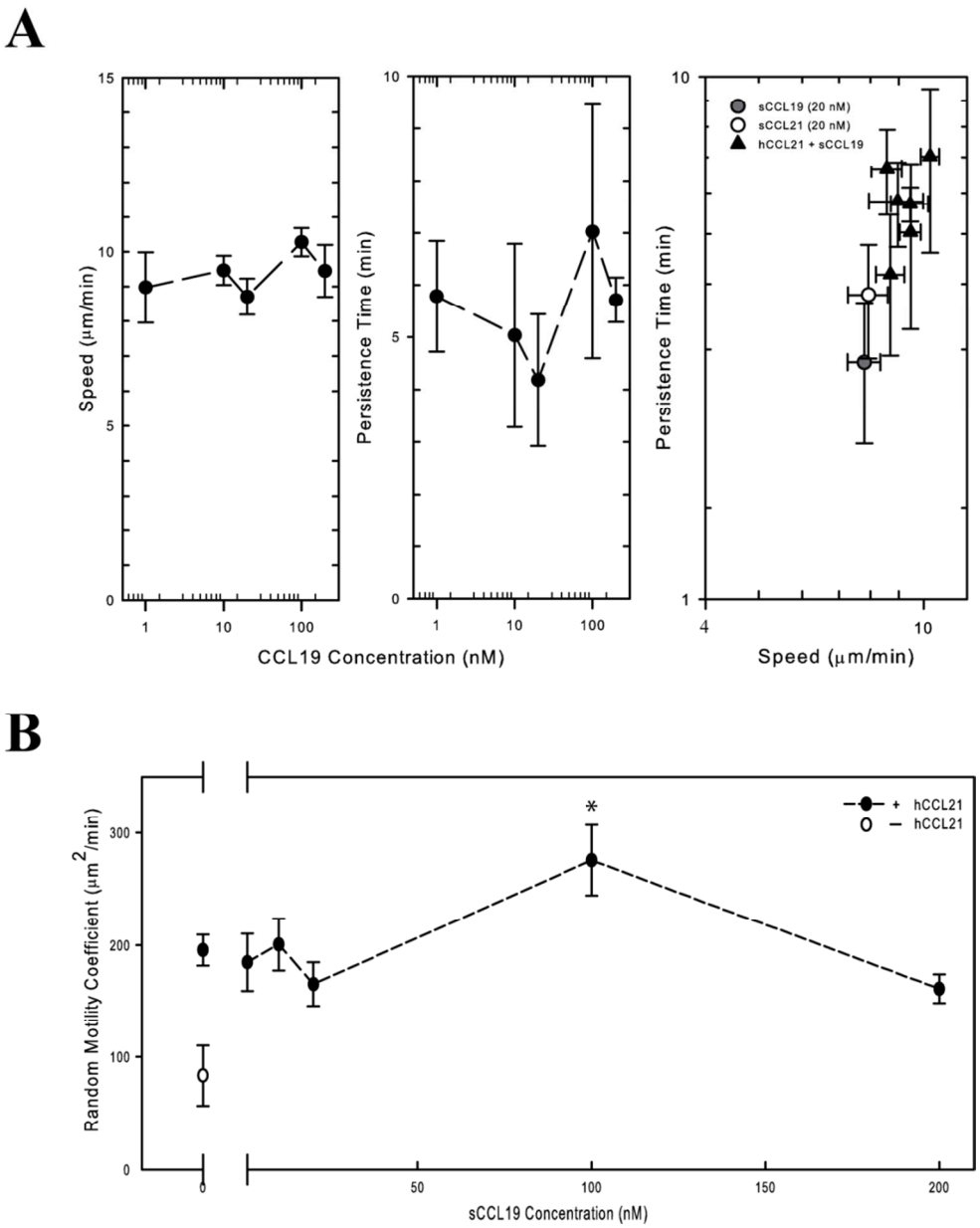

Fig. 6 hCCL21 and sCCL19 induce chemokinesis on *low* ICAM-1 surfaces. (A) T lymphocyte speeds and persistence times on hCCL21 and varying sCCL19 concentrations (left two panels); speed remains constant with a peak in persistence time at 100 nM sCCL19. The right graph indicates a loss of the inverse correlation between speed and persistence time. (B) Peak in hCCL21 and sCL19 chemokinesis at 100 nM sCCL19 with the highest observed $\mu = 275.63 \pm 31.3\ \mu m^2/min$; *$p < 0.05$, compared to no CCL21; one-sample t test The error bars represent the standard error of the mean (s.e.m.)